UNIVERSITYOF BIRMINGHAM

Research at Birmingham

Analysis of stroboscopic signal sampling for radar target detectors and range finders

Bystrov, Aleksandr; Gashinova, Marina

Document Version
Publisher's PDF, also known as Version of record

Link to publication on Research at Birmingham portal

Analysis of stroboscopic signal sampling for radar target detectors and range finders

Aleksandr Bystrov, Marina Gashinova

EECE, University of Birmingham, Birmingham, B15 2TT, UK
E-mail: m.s.gashinova@bham.ac.uk

Abstract: This study considers the influence of signal sampling on the characteristics of target detectors and range finders, which form parts of radar systems. Quasi-optimal algorithms for target detection and range measurement are analysed, which demonstrate close to optimal performance even if low-performance signal processing equipment is used. Special attention is given to stroboscopic sampling. In the case of a high signal-to-noise ratio, stroboscopic sampling can provide better detection performance than traditional, or real-time, sampling. The accuracy of range finders with stroboscopic signal sampling is estimated. The considered method allows for a reduction in both instrumental range measurement error and random error of tracking compared with traditional sampling methods, without an increase in requirements of the range finders' performance.

1 Introduction

In ultra-wideband radar systems, limited system performance can prevent the use of optimal algorithms of real-time digital signal processing [1]. This paper considers the quasi-optimal algorithms of target detection and range measurement, which demonstrate near optimal characteristics when using low-rate signal sampling.

In order to increase radar system performance, parallel sampling and parallel data processing can be used [2, 3]. However, such methods lead to significantly higher hardware costs. In this paper, we will focus on algorithms that provide higher radar system performance at a low cost. Such algorithms include:

- low-digit (including binary) signal and coefficients quantisation [4, 5];
- under sampling, that is, the sampling below the Nyquist frequency [5, 6];
- algorithms of a quasi-optimal signal filtering [7];
- special methods of reducing instrumental range measurement errors, including two-step range estimation (rough and precise) [5], the vernier method [8] and stroboscopic sampling (use of sliding time samples) [2, 9].

In this paper, we will analyse the influence of sampling frequency on the characteristics of target detectors and range finders as well as the characteristics of target detectors and range finders with stroboscopic sampling. Finally, recommendations for the practical use of stroboscopic signal sampling are developed.

The remainder of this paper is organised as follows. In Section 2, the radar target detector with a stroboscopic signal sampling algorithm is described and the detection performance is estimated; Section 3 presents a radar range finder that utilises stroboscopic sampling, together with analysis and characteristics; simulation results are presented in Section 4 and the conclusion is formulated.

2 Radar target detectors

The optimal algorithm for detecting a pulsed signal in a background of stationary noise with a random, but the known power spectral density or autocorrelation matrix, represents a calculation of the correlation integral of the received signal within each range resolution cell and compares it to the threshold, which is specified according to the desired false alarm probability [10].

2.1 Real-time signal sampling

Let us start with an analysis of real-time signal sampling, that is, sampling at the Nyquist rate. If the number of pulses in a train is not too large, but sufficient for target detection in many practical cases (several hundred), the optimal algorithm of detection can be implemented using modern digital signal processors [11]. For the processing of a larger number of pulses, it is possible to use multiprocessor systems or quasi-optimal algorithms, that is, simplified optimal detection algorithms where the symmetry of the signal envelope and equilibrium summing of signal samples are assumed. This allows for the enhancement of the target detector's performance.

To answer the question of the quality of the quasi-optimal digital target detectors, the power losses because of signal sampling have to be investigated.

For the analysis of target detector performance it is usually assumed that the noise on its input is normally distributed [12]

$$p_\xi(u) = \frac{1}{\sigma_\xi \sqrt{2\pi}} \exp\left(-\frac{u^2}{2\sigma_\xi^2}\right) \quad (1)$$

where σ_ξ^2 is the variance of the noise. In case of matched filtering of a rectangular pulse, the input signal has a triangular shape

$$u(t) = \begin{cases} U(1 - |t|/\tau), & \text{if } |t| < \tau \\ 0, & \text{if } |t| \geq \tau \end{cases} \quad (2)$$

with an amplitude of the maximum signal samples distributed according to the expression

$$p_s(u) = \begin{cases} \dfrac{2}{T}\dfrac{\tau}{U}, & \text{when } U\left(1 - \dfrac{T}{2\tau}\right) < u < U \\ 0, & \text{when } u \geq U \text{ or } u \leq U\left(1 - \dfrac{T}{2\tau}\right) \end{cases} \quad (3)$$

where U is the signal amplitude, T is the sampling interval and τ is the pulse width, as illustrated in Figs. 1a–c.

The real-time signal sampling causes the reduction in the signal-to-noise ratio (SNR), which can be estimated by comparing the signal amplitude U with the mean value of the signal sample nearest to the maximum

$$\rho = 1 - \frac{T}{4\tau} \quad (4)$$

Therefore with five or six samples per signal, the losses do not exceed 10%, which is acceptable for many practical cases. In case of insufficient performance of the target detector, the maximum achievable number of samples can be less than 5 or 6. In Section 2.2, the stroboscopic sampling will be considered, which allows improvement of the detection characteristics in low-performance detector.

The key characteristics of target detection are detection probabilities and false alarm rates. For the development of quasi-optimal target detection algorithms, the effect of the
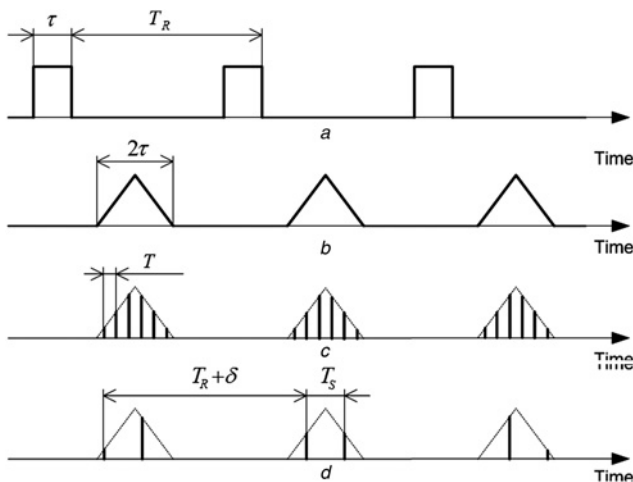
signal sampling rate on these characteristics should be evaluated.

In this paper, the detection characteristics for a non-fluctuating or a slowly fluctuating signal will be obtained. This assumption is applicable for cases where the scattering surface of the target changes slightly between pulses. The probability density function of the signal and noise compound is given as a convolution

$$p_{s\xi}(u) = \int_{-\infty}^{\infty} p_\xi(u - x)p_s(x)\,\mathrm{d}x \quad (5)$$

Substituting (1) and (3) into (5), we can obtain

$$p_{s\xi}(q) = \frac{2\tau}{TU}\left\{\Phi(q - \lambda) - \Phi\left[q\left(1 - \frac{T}{2\tau}\right) - \lambda\right]\right\} \quad (6)$$

where

$$\Phi(x) = \frac{1}{\sqrt{2\pi}}\int_{-\infty}^{x} \mathrm{e}^{-t^2/2}\,\mathrm{d}t \quad (7)$$

is the probability integral, $q = U/\sigma_\xi$ is the SNR, $\lambda = u/\sigma_\xi$ is the relative threshold defining the false alarm probability [10]

$$P_{FA} = 1 - \Phi(\lambda) \quad (8)$$

The detection probability is then defined as

$$P_D = \int_{\lambda}^{\infty} p_{s\xi}(q)\,\mathrm{d}q \quad (9)$$

Expression (9) allows for finding the detection probability against SNR with a fixed false alarm rate P_{FA} for the considered detector (Fig. 2). The curves shown in Fig. 2 as dashed lines correspond to the case of one sample per pulse in real-time sampling, that is, $T = 2\tau$ (values q are given in an absolute scale). The characteristics of an analogue detector for the known signal detection [10] are shown here as dotted lines. The detection characteristics in case of stroboscopic sampling, which will be considered further in the paper, are shown as solid lines.

Fig. 1 *Signal representation in the impulse radar*

a Transmitted train of pulses
b Received pulses
c Real-time sampling
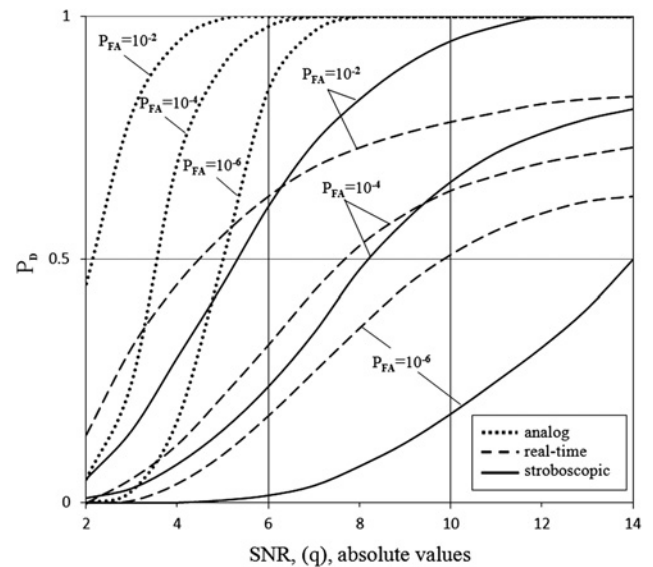*d* Stroboscopic sampling of the received signal

Fig. 2 *Detection performance of analogue and digital target detector*

In order to ensure the same detection probability as in the case of an analogue detector, it is necessary to increase the SNR. For example, for $P_D = 0.5$ and $P_{FA} = 10^{-4}$, SNR should be increased from 3.3 to 7.5 and, moreover, P_D is limited by about 0.75 even at $q = 14$.

2.2 Stroboscopic signal sampling

Real-time sampling requires the use of a high-speed analogue-to-digital converter, which can be both expensive and power consuming. To increase the performance of the detector, stroboscopic sampling of signals [13] can be exploited. The procedure is illustrated in Fig. 1d. This method leads to the increasing of target detection time by taking smaller number of samples for each received pulse, but after every pulse repetition interval T_R the sampling time should have a small offset

$$\delta = T_S/N \qquad (10)$$

where N is the number of transmitted pulses needed to build the signal profile and T_S is the stroboscopic sampling interval. The implementation of stroboscopic sampling does not require additional hardware and it is only necessary to provide sampling frequency stability (low clock drift) [14].

Furthermore, we will show that detectors with stroboscopic sampling can provide better detection performance than detectors with traditional sampling in the case of small numbers of samples within the pulse. We will consider the maximum amplitude signal sample that is closest to the centre of the pulse, its distance from the centre of the signal is equal to ϑ and the probability density equals to

$$p(\vartheta) = \begin{cases} 1/T, & \text{if } \vartheta| < T/2 \\ 0, & \text{if } \vartheta| \geq T/2 \end{cases} \qquad (11)$$

For stroboscopic sampling with large N the sum of signal samples, which are uniformly distributed on the interval $[(\vartheta - T/2), (\vartheta + T/2)]$, will be close to the average value of the signal envelope

$$\overline{u}(\vartheta) = \frac{1}{T_S} \int_{\vartheta - T/2}^{\vartheta + T/2} u(t)\, \mathrm{d}t$$

Let us consider a case of one sample per pulse, that is, $T_S = T = 2\tau$. Substituting the expression for the envelope of the signal and calculating the integral from $\vartheta - T/2$ to 0 and then from 0 to τ, we obtain

$$\overline{u}(\vartheta) = U \left(\frac{1}{2} - \frac{\vartheta^2}{4\tau^2} \right) \qquad (12)$$

The average reduction in the SNR for the considered case of stroboscopic sampling exceeds the corresponding values (4) of the traditional (real-time) sampling

$$\rho = \frac{1}{TU} \int_{-T/2}^{+T/2} \overline{u}(\vartheta)\, \mathrm{d}\vartheta = 1 - \frac{T}{3\tau} \qquad (13)$$

However, even in this case the stroboscopic sampling can provide better results than the traditional sampling.

Calculating $p_S(\overline{u}) = 2p(\vartheta) |(\mathrm{d}\,\vartheta(\overline{u}))/(\mathrm{d}\,\overline{u})|$ and substituting (1) into (5) we obtain an expression for the probability

density of the signal and noise compound $p_{s\xi}(q)$ in case of stroboscopic sampling and to obtain P_{FA} and P_D by (8) and (9).

In Fig. 2, the detection performance in case of stroboscopic sampling is shown (solid lines) in addition to the previously considered analogue and traditional sampling. It is clear that the stroboscopic sampling has an advantage to traditional sampling in cases when it is necessary to provide a high detection probability. For example, when $P_D = 0.8$ and $P_{FA} = 10^{-2}$, this method requires approximately 1.5 times less SNR.

Thus, the analysis of the detection performance shows that the stroboscopic sampling has an advantage over the traditional sampling in terms of SNR when the sampling period is equal to or exceeds the pulse duration. In the case of small values of threshold λ, or a high acceptable probability of false alarm, the detection probability for a given SNR value in the target detector with stroboscopic sampling is higher than in the detector with traditional sampling.

3 Range finders

When a target is detected, the range finder should provide the distance to the target. The radar range finder represents a non-linear discrete automatic tracking system, the behaviour of which depends on the parameters of signal digitising. The range finder block diagram is shown in Fig. 3 and consists of a delay measuring system, a low-pass filter and a gate generator producing a reference signal with the delay, which is proportional to the low-pass filter output signal delay. The optimum delay measuring system contains an optimum time gate and integrator, or generalised time discriminator.

Range tracking is carried out in pulsed radar by the direct matching of a range gate position to the delayed echo pulse. The usual technique is a split gate range tracker, which is a form of range tracker with a pair of time gates called an early gate and a late gate, contiguous or partly overlapping in time [10, 12]. Deviation of the pair of gates from the proper tracking position increases the signal energy in one gate and decreases it in the other, producing an error signal. The range difference channel is formed by subtracting the late gate output from the early gate output and integrating the result, to form a time discriminator response. The error signal from the discriminator provides the input to an electronic tracking loop that controls the timing of the gates.

3.1 Losses because of real-time signal sampling

In order to analyse the impact of signal digitising on the characteristics of the time discriminator, we will consider the time discriminator based on the early and late gate techniques. Although the discriminator characteristic is nonlinear in general, the discriminator will operate in its linear regime if the difference between the estimated delay and the true delay (delay measurement error) is small.
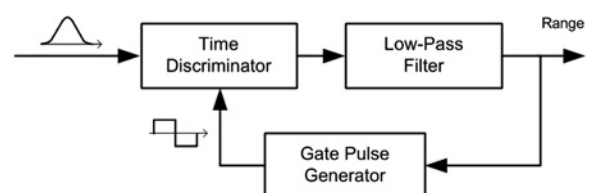

Fig. 3 *Range finder block diagram*

In the considered case of matched filtering of the rectangular pulse the number of samples per each pulse is equal to

$$n = 2\tau/T \tag{14}$$

The signal at the time discriminator output in case the time delay measurement error equals $j \cdot T$ is

$$Q(jT) = -\sum_{i=j}^{j+n/2-1} u(iT) + \sum_{i=j+n/2}^{j+n-1} u(iT), \tag{15}$$
$$j = 0, \pm 1, \pm 2\ldots$$

where $u(iT)$ are samples of the input signal. Therefore if $j = 0$ (zero error)

$$Q(0) = -\sum_{i=0}^{n/2-1} u(iT) + \sum_{i=n/2}^{n-1} u(iT) \tag{16}$$

Assuming that at the input of the discriminator there is only a stationary Gaussian noise with a variance σ_ξ^2, the value of the output noise is equal to

$$\sigma_{\xi\_out}^2 = \overline{[Q(0)]^2} \tag{17}$$

Substituting (16) into (17) after appropriate calculations [15] we can obtain

$$\sigma_{\xi\_out}^2 = \sigma_\xi^2 \varphi(n, r) \tag{18}$$

In (18), the function $\varphi(n, r)$ describes the dependence of the output noise on the number of samples per pulse and on the autocorrelation properties of the input noise

$$\varphi(n, r) = n + 4\sum_{i=1}^{n/2-1}\left(\frac{n}{2} - i\right)r(iT) - 2\sum_{i=1}^{n/2} ir(iT)$$
$$- 2\sum_{i=1}^{n/2-1}\left(\frac{n}{2} - i\right)r\left[\left(\frac{n}{2} + i\right)T\right] \tag{19}$$

where $r(iT)$ is the normalised autocorrelation function of input noise, defined by the amplitude–frequency response characteristic of the radar receiver.

In the linear model the time discriminator can be presented by the linear gain term with a steepness of $K_d = ((dQ(x))/(dx))\big|_{x=0}$. In the considered case of matched filtering, the input signal has a triangular shape with the amplitude U

$$K_d = 2Uk_d \tag{20}$$

where $k_d = 0.5n/\tau$. In order to compare the digital time discriminator with the analogue device, expression (18) may be rewritten as

$$\sigma_{\xi\_out}^2 = 2\sigma_\xi^2 k_d^2 \tau^2 \vartheta(n, r) \tag{21}$$

where

$$\vartheta(n, r) = 2\varphi(n, r)/n^2 \tag{22}$$

Since the model is linear, the noise can be recalculated at the input of the discriminator after scaling by the discriminator steepness $\sigma_{\xi\_in}^2 = \sigma_{\xi\_out}^2/K_d^2$. Comparison with the analogue device [15] shows that signal sampling leads to an increase of output noise in the case of the digital range finder. The digital discriminator losses are illustrated in Fig. 4 for the case where the equivalent bandwidth of the receiver is matched to the pulse duration. When the number of samples per pulse is more than six, the losses do not exceed 1 dB. Thus, to reduce the losses in SNR because of sampling, it is necessary to increase the number of samples per pulse, that is, the sampling rate.

3.2 Stroboscopic sampling errors

3.2.1 Instrumental errors: A higher sampling rate leads not only to the increase of SNR, but also to the decrease of the instrumental error of the range measurement in digital range finders, which can significantly degrade the accuracy of tracking. Instrumental errors are because of the finite resolution of the digital representation of the range and are the difference between the exact range and the digitised range. An instrumental error can be considered as additional noise because of its stochastic behaviour. It varies from $-T/2$ to $T/2$ at the discriminator input; therefore its variance is [16]

$$\sigma_i^2 = T^2/12 \tag{23}$$

For the reduction of instrumental errors it is necessary to increase the sampling rate. The use of stroboscopic sampling allows for achieving similar results as with an increase in the sampling rate but without any higher requirements to the digital range finders' performance. The instrumental error decreases when the number of transmitted pulses needed to build the signal profile increases. From expressions (10), (14) and (23), we can derive the instrumental error in case of stroboscopic sampling

$$\sigma_i^2 = \frac{\delta^2}{12} = \frac{\tau^2}{3n^2N^2} \tag{24}$$

Despite the obvious advantage of lowering the instrumental error in range measurement, stroboscopic sampling has a number of inherent shortcomings. Further on we will
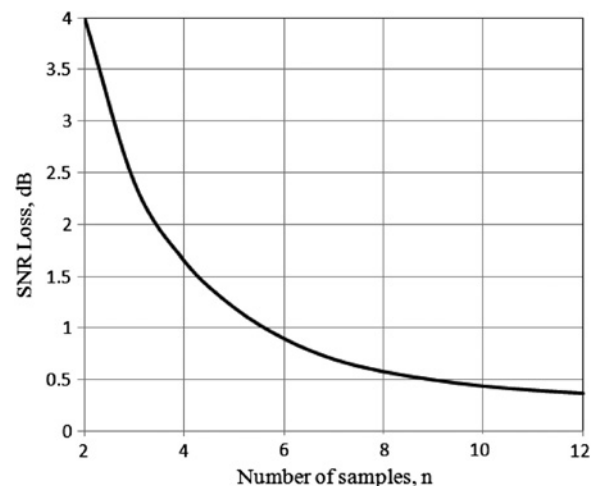

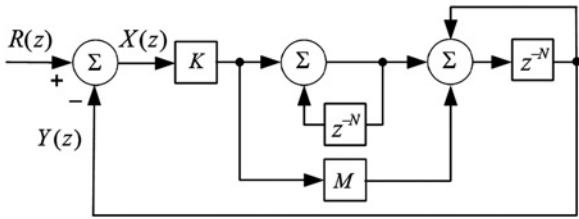**Fig. 4** *SNR loss because of signal sampling*

Fig. 5 *Block diagram of range finder with stroboscopic sampling*

consider and discuss the dynamic error and the additional range measurement errors, such as errors because of target fluctuation, target shift and input noise in case of stroboscopic sampling.

3.2.2 Dynamic errors:
Dynamic errors occur because of the inability of the radar to follow the target echo accurately and depend on target speed, acceleration and the parameters of the range finder. Generally, the Wiener filter is widely used in tracking systems, with constant coefficients providing a minimum of a root mean square error of tracking in static mode [17]. It provides a zero dynamic error of tracking in the case of object movement with constant speed and a constant dynamic error in the case of object movement with constant acceleration.

The range finder can be analysed using standard discrete-time analysis (i.e. z-transform) techniques [16]. A block diagram of the considered range finder with stroboscopic sampling utilising a Wiener filter of a second order is shown in Fig. 5, where $R(z)$ is the actual distance to the target, $Y(z)$ is the estimated distance, $X(z)$ is the measurement error, K is the feed-forward coefficient (gain) and M is the feed-backward coefficient, defined by filter parameters.

Using final value theorem [1] we can express the dynamic error as

$$m_x = \lim_{z \to 1}(z-1)X(z) = \lim_{z \to 1}(z-1)R(z)\big[1 - K_c(z)\big] \quad (25)$$

where $K_c(z)$ is the transfer function of a closed-loop tracking system. The closed-loop transfer function $K_c(z)$ can be calculated from the open-loop transfer function $K_o(z)$ as [1] $K_c(z) = K_o(z)\,[1 + K_o(z)]$.

If we consider the range finder in Fig. 5 as a series of interconnections of the two first-order systems, the open-loop and closed-loop transfer functions of the tracking system with stroboscopic sampling can be expressed in accordance with the general rules of z-transform as

$$K_o(z) = \frac{K\big[z^N(M+1) - M\big]}{(z^N - 1)^2} \quad (26)$$

$$K_c(z) = \frac{K\big[z^N(1+K) - M\big]}{z^{2N} + z(K + KM - 2) + 1 - KM} \quad (27)$$

When the target moves with constant acceleration a the distance to it changes with time as $r(t) = at^2/2$. Its z-transform is, therefore $R(z) = \big((aT_R^2)/2\big)\big(z(z+1)/(z-1)^3\big)$. From (25)–(27), we can obtain the dynamic error

$$m_x = \frac{a(NT_R)^2}{K} \quad (28)$$

This equation shows that stroboscopic sampling leads to an increase of the dynamic error in N^2 times in comparison with real-time sampling for which $N = 1$.

3.2.3 Stochastic errors:
Let us now consider the stochastic errors of range measurement in range finders with stroboscopic signal sampling. This error occurs even at a zero-tracking error because of target fluctuation so that the output value of the discriminator will be non-zero. Indeed, since the amplitude of the signal changes from scan to scan, its envelope, restored after the stroboscopic sampling, will be distorted. Consequently, the signal energy in the gates will be different. In this paper, only simplified target model is analysed, which does not consider the range fluctuation of the target.

The variance of the stochastic range measuring error can be expressed [12] as

$$\sigma_x^2 = S_\xi(0)f_e \quad (29)$$

where $S_\xi(0)$ is the noise spectrum density at zero frequency and

$$f_e = \frac{1}{2\pi}\int_{-\pi/T_r}^{\pi/T_r} \big|K_c(j\omega)\big|^2 \, d\omega \quad (30)$$

is the equivalent bandwidth of the closed-loop tracking system, $K_c(j\omega)$ is the transfer function of the closed-loop tracking system and ω is the angular frequency.

The equivalent bandwidth of the closed-loop tracking system shown in Fig. 5 is therefore

$$f_{eS} = \frac{1}{NT_R}\frac{2/M + K(1 + 2M)}{4 - K(1 + 2M)} \quad (31)$$

A minimum of f_{eS} is achieved at $M = 1/\sqrt{K} - 0.5$

$$f_{eS,\,min} = \frac{\sqrt{K}}{NT_R}\frac{4 - \sqrt{K}}{(2 - \sqrt{K})^2} \quad (32)$$

Firstly, let us consider the impact of target fluctuation on the accuracy of tracking. The signal amplitude is distributed according to Rayleigh [18], with a variance of amplitude fluctuation of input signal σ_a^2 and the correlation coefficient $r_a(t) = \exp(-|\tau|/\tau_a)$, where the correlation time of amplitude fluctuation is $\tau_a \le NT_R$. At higher τ_a the fluctuation will have no effect on the characteristics of the time discriminator and the signal can be considered as non-fluctuating.

Similar to (16), we can express the output signal of the stroboscopic time discriminator based on the early and late gate algorithms as

$$Q_S(0)$$

$$= -\sum_{j=0}^{N-1}\left[\sum_{i=0}^{(n/2)-1} u\big(jT_R + iT + j\delta\big) - \sum_{i=n/2}^{n-1} u\big(jT_R + iT + j\delta\big)\right] \quad (33)$$

This expression can be simplified, taking into consideration

that

$$u\left(jT_R + iT + j\delta\right) = a\left(jT_R\right)u\left(iT_R + j\delta\right) = a_j u_{ij} \quad (34)$$

where $u(iT + j\delta) = u_{ij}$ is the signal envelope and $a(jT_R) = a_j$ is the random amplitude fluctuation in sounding pulse periods. Therefore

$$Q_S(0) = -\sum_{j=0}^{N-1} a_j \left(\sum_{i=0}^{n/2-1} u_{ij} - \sum_{i=n/2}^{n-1} u_{ij}\right) \quad (35)$$

The expression in brackets represents the output of the discriminator in jth period. Since the difference between the estimated and the true distance to the target within the jth period can be expressed as $e_j = (N - 2j - 1)\delta$, (35) can be reduced to

$$Q_S(0) = -\sum_{j=0}^{N-1} a_j\left(K_{dS} e_j\right) \quad (36)$$

where the discriminator steepness K_{dS} similar to (20) is $K_{dS} = 2Uk_{dS}$ and the sampling discriminator gain in case of stroboscopic sampling is $k_{dS} = 0.5 \times nN/\tau$. The variance of the tracking error in this case is

$$\sigma_{a\_out}^2 = \overline{Q_S(0)^2} = 4\sigma_a^2\,\tau^2 k_{dS}^2\,\psi(N)/n^2 \quad (37)$$

In (37) $\psi(N)$ describes the dependence of the tracking error on the number of transmitted pulses used to build the signal profile

$$\psi(N) = \frac{1}{N^2\sigma_a^2}\overline{\left(\sum_{j=0}^{N-1} a_j \frac{N - 2j - 1}{N} U\right)^2} \quad (38)$$

Besides its dependence on N, the function $\psi(N)$ (38) is determined by the value of the relative correlation interval of fluctuations $\mu = \tau_a/T_R$. Indeed, in the calculations of this formula, $\overline{a_j a_{j+L}} = \sigma_a^2 r_a(L\,T_R/\tau_a) = \sigma_a^2 \exp(-L/\mu)$. The diagrams $\psi(N)$ are illustrated in Fig. 6. For each N the increase in the number of samples n per pulse leads to the decrease of the sampling interval T, and therefore to the reduction of influence of target fluctuation. When $\tau_a \gg T_R$,
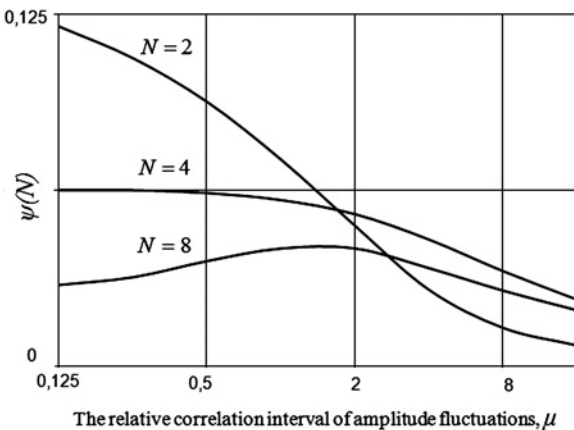

Fig. 6 *Influence of target amplitude fluctuation on the characteristics of time discriminator in case of triangular signal envelope and n = 2*
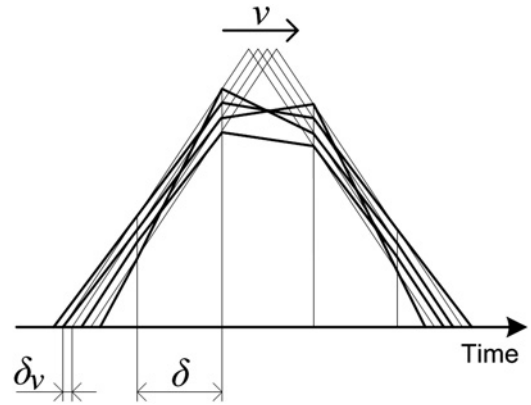
Fig. 7 *Distortion of signal envelope (N = 4, n = 1)*

the signal can be considered non-fluctuating and $\psi(N)\simeq0$. In case of small values of μ the samples in the adjacent periods of sounding are not correlated and $\psi(N)\simeq1/(n^2N)$. If we recalculate the noise to time discriminator input $\sigma_{a\_in}^2 = \sigma_{a\_out}^2/K_{dS}^2$, we will find that the maximum variance of target fluctuation noise is

$$\sigma_{a\_in}^2 \simeq \frac{\tau^2}{4n^2N} \quad (39)$$

The stochastic component of the range measurement error caused by target fluctuation is determined by the formula

$$\sigma_{xa}^2 = \sigma_{a\_in}^2 f_e T_R \quad (40)$$

where f_e is the equivalent bandwidth of a closed-loop tracking system (31) at $N = 1$. The second cause of stochastic tracking error is because of target motion. The target shift in range measurements within each cycle of stroboscopic sampling leads to the distortion of the signal envelope, built as a result of stroboscopic sampling [19].

The signal envelopes in the four adjacent cycles of stroboscopic sampling are shown in Fig. 7. The target shift is $\delta_v = 2vT_R/c$, where v is the target speed and c is the speed of light in free space. The solid lines are the envelopes of the signal, recovered as a result of stroboscopic sampling. It shows that the shape deviation from the triangle has a stochastic character, since the position of the samples depends on the actual range and can be considered accidental. Therefore the influence of this effect can be considered as an additional measurement error.

If we consider the envelope of the signal averaged over N realisations, its duration will be equal to the duration of the original signal though the maximum value will be lower than the amplitude of the original signal. Instantaneous values of the signal $\bar{u}(t)$ are within the range $u(t) - \left((U\delta_v)/(n\delta)\right) \leq \bar{u}(t) \leq u(t) + \left((U\delta_v)/(n\delta)\right)$. Such a distortion of the envelope waveform leads to the reduction of the discrimination characteristic gain

$$k_{dS} = k_d\left(1 - \frac{\delta_v}{2n\delta}\right) \quad (41)$$

It is clear that dynamic errors will increase with gain decrease. In an unfavourable case, when tracking is still possible, that is, when the target moves during measurement on a

distance equal to the length of a pulse $N\delta_v = \tau$, the gain will decrease approximately by a third: $k_{dS} \simeq 0.75 k_d$.

The effect of this distortion is equivalent to the appearance of additional noise at the output of the time discriminator. Assuming that noise amplitudes are randomly distributed, the variance of this noise can be written as

$$\sigma_{v\_out}^2 = \frac{N}{3}\left(\frac{U\delta_v}{n\delta}\right)^2 \qquad (42)$$

If we recalculate the noise to the discriminator input $\sigma_{v\_in}^2 = \sigma_{v\_out}^2 / K_{dS}^2$ using (41), we will receive the expression for the variance of the equivalent noise

$$\sigma_{v\_in}^2 = \frac{1}{\chi^2}\frac{\tau^2}{N} \qquad (43)$$

where

$$\chi^2 = 3n^2\left(\frac{2n\delta}{\delta_v} - 1\right)^2 \qquad (44)$$

In the most unfavourable case, when $N\delta_v = \tau$ and $n = 1$, given the fact that $\delta = 2\tau/(nN)$, we get $\chi^2 = 27$. Therefore the maximum variance of the input noise is

$$\sigma_{v\_in}^2 = \frac{\tau^2}{27N} \qquad (45)$$

The stochastic component of the range measurement error caused by target motion can be determined by the formula

$$\sigma_{xv}^2 = \sigma_{v\_in}^2 f_e T_R \qquad (46)$$

Let us now consider the third cause of the stochastic tracking error – the error caused by stationary Gaussian input noise with a variance σ_ξ^2. The stroboscopic time discriminator algorithm is expressed in (33). Making some manipulations similar to that used for the derivation of (18) and (19), and assuming that the noise values separated by intervals T_R are uncorrelated, we obtain the value of the output noise

$$\sigma_{\xi S\_out}^2 = 4\sigma_\xi^2 k_{dS}^2 \tau^2 \varphi_S(n, r)/N \qquad (47)$$

In (45), the function $\varphi_S(n, r)$ describes the dependence of the output noise on the number of samples per pulse and the autocorrelation properties of the input noise. Similar to (19) it can be expressed as

$$\varphi_S(n, r) = n + 4\sum_{i=1}^{n/2-1}\left(\frac{n}{2} - i\right)r(i\delta) - 2\sum_{i=1}^{n/2} ir(i\delta)$$
$$- 2\sum_{i=1}^{n/2-1}\left(\frac{n}{2} - i\right)r\left[\left(\frac{n}{2} + i\right)\delta\right] \qquad (48)$$

In case of $N > 4$ $\varphi_S(n, r) \simeq 0.425$ [15] and expression (47) can be simplified

$$\sigma_{\xi S\_out}^2 \simeq \sigma_\xi^2 k_d^2 \tau^2 / N \qquad (49)$$

Again, recalculating noise to the discriminator input its

variance $\sigma_{\xi S\_in}^2 = \sigma_{\xi S\_out}^2 / K_{dS}^2$ will be

$$\sigma_{\xi S\_in}^2 = \frac{1}{\rho^2}\frac{\tau^2}{4N} \qquad (50)$$

where $\rho = U/\sigma_\xi$ is the input SNR.

Thus the stochastic component of the range measurement error caused by input noise is

$$\sigma_{x\xi}^2 = \sigma_{\xi S\_in}^2 f_e T_R \qquad (51)$$

If we compare (50) with (39) we can see that target fluctuations in the most unfavourable cases are equivalent to the presence of input noise with SNR $\rho = n$. By comparing (50) with (45), we can conclude that the maximum range measurement error caused by target movement is equivalent to the presence of input noise with SNR$\rho \simeq 2.6$.

Finally, the range measuring error is defined by both the dynamic error m_x and the root mean square value of the stochastic error

$$\sigma_x = \sqrt{\sigma_i^2 + \sigma_{xa}^2 + \sigma_{xv}^2 + \sigma_{x\xi}^2} \qquad (52)$$

4 Example of a range finder performance

Radar range finders with stroboscopic sampling allow for reducing the instrumental range measurement error at the cost of an increased dynamic error. Therefore stroboscopic sampling is effective in case of a small dynamic error and big instrumental errors of the initial system, that is, the range finder without stroboscopic sampling. In order to illustrate this we will consider the range finder intended for tracking, if not manoevring, high speed objects. Let us assume that target fluctuations are insignificant, that is $\sigma_{xa} = 0$.

The range to the target changes from the starting value to the minimum distance defined at the moment of the greatest convergence of the target to the radar r_1 (about 30 m). We will consider an example where the pulse duration $\tau = 30$ ns, the pulse repetition period $T_R = 10 \mu$s, SNR = 20 dB, target fluctuation is insignificant and its speed $v = 3.5$ km/s.

The radial acceleration of the object reaches maximum at the time of closest approach to the radar $a(r_1) = v^2/r_1 = 41$ km/s². In the example, we will consider one sample per pulse and the range finder having coefficients $K = M = 1$.

A maximum dynamic error can be obtained from (26): $m_x = a(r_1)(NT_R)^2$. From (50) and (51) we will define the variance of the input noise error $\sigma_{x\xi}^2$. The variance of the instrumental error (24) in the considered case is $\sigma_i^2 = \tau^2/(3N)$. The variance of the error caused by signal envelope distortion because of the target motion shift σ_{xv}^2 can be defined by (43)–(46). The results of the calculations are illustrated in Fig. 8, which shows the dependence of each error on the number of pulses.

The figure demonstrates that the number of periods N of stroboscopic sampling affect the stochastic errors in different ways: if with the increase of N the instrumental error σ_i quickly decreases, the error caused by target shift σ_{xv} grows slowly. Therefore in case of $N > 10$, the main contribution in the overall stochastic error σ_x is because of the noise error component $\sigma_{x\xi}$, which decreases more slowly than σ_i.

There are two clear opposite trends for the dynamic and stochastic errors. While N is below 40–50, the range
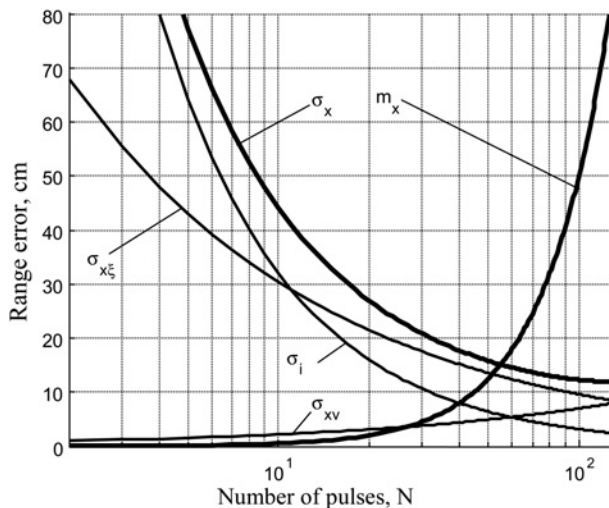
Fig. 8 *Dependence of range finder errors on the number of pulses in the case of stroboscopic sampling*

measurement error is defined chiefly by the stochastic error which is generally inversely proportional to N.

When $N > 60$, the dynamic error that increases proportionally to N^2 will mainly contribute to the overall system error in the case of stroboscopic sampling. Therefore there is an optimal value of N which corresponds to the intersection of the stochastic and dynamic error plots. In the considered case the maximum accuracy of tracking is reached when $N = 64$.

The described algorithms with the stroboscopic sampling have been used in practical range finder systems [20] and the experimental results agree well with all estimations made.

5   Conclusions

This paper has focused on the detailed analysis of stroboscopic sampling for digital radar target detectors and range finders and its performance in cases when it is difficult to provide the required high sampling rate of real-time signal sampling.

We have shown that stroboscopic sampling may provide better detection performance for target detectors than traditional sampling in cases where the number of samples per pulse duration is small (two or less). We have also demonstrated that the advantages of stroboscopic sampling become greater with an increase of SNR.

An analysis of the characteristics of the range finder with stroboscopic signal sampling has shown that this technique allows for reducing the instrumental range measurement error without increasing the requirements of the digital range finders' performance. The presented results demonstrate how to define optimal stroboscopic sampling parameters in order to provide maximum accuracy of range tracking.

6   References

1   Kuo, S.M., Lee, B.H.: 'Real-time digital signal processing', (John Wiley & Sons Ltd, 2001)
2   Findlay, A.M., Ornstein, E.: 'Sampling wideband, non-repetitive radar signals'. Proc. IEEE Int. Radar Conf., Arlington, Virginia, 1975, pp. 288–293
3   Shi, G., Liu, Z., Chen, X.Y., Wang, L.J.: 'A parallel sampling scheme for ultra-wideband signal based on the random projection'. Proc. IEEE Int. Symp. ISCAS, 2008, pp. 2246–2249
4   Bar-Shalom, O., Weiss, A.J.: 'DOA Estimation using one-bit quantized measurements', *IEEE Trans. Aerosp. Electron. Syst.*, 2002, **38**, (3), pp. 868–884
5   Gezici, S., Poor, H.V.: 'Position estimation via ultra-wide-band signals', *Proc. IEEE*, 2009, **97**, (2), pp. 386–403
6   Mishali, M., Eldar, Y.C.: 'From theory to practice: sub-Nyquist sampling of sparse wideband analog signals', *IEEE J. Sel. Top. Signal Process.*, 2010, **4**, (2), pp. 375–391
7   Chernoguz, N.: 'Adaptive range tracking for radar technique'. Proc. 2011 IEEE Radar Conf. (RADAR), 2011, pp. 189–194
8   Lu, Y.H., Ng, C.S., Zhang, C.B., Yao, T.S.: 'An advanced vernier method for accurate radar ranging'. Proc. Geoscience and Remote Sensing Symposium IGARSS '93, 1993, **4**, pp. 2040–2042
9   Hamran, S.-E.: 'Radar performance of ultra wideband waveforms', in Kounemou, G. (Ed.): 'Radar technology' (INTECH, 2009)
10 Skolnik, M.I.: 'Radar handbook', (McGraw-Hill, 2008, 3rd edn.)
11 Djigan, V.I., Bystrov, A.N.: 'Cost effective algorithms in radar detectors and range finders', *J. Radio Electron., Gen. Tech. Ser. (Russia)*, 2011, **1**, pp. 114–124
12 Barton, D.K., Ward, H.R.: 'Handbook of radar measurement' (Prentice-Hall, 1969)
13 Howard, D.D.: 'High range resolution monopulse tracking radar', *IEEE Trans. Aerosp. Electron. Syst.*, 1975, **11**, (5), pp. 749–755
14 Wang, Y., Leus, G., Delic, H.: 'TOA estimation using UWB with low sampling rate and clock drift calibration'. Proc. IEEE Int. Conf. Ultra-Wideband, 2009, pp. 612–617
15 Nezlin, D.V., Bystrov, A.N.: 'Characteristics of time discriminator with stroboscopic radar signal sampling', *Radiotechnika (Russia)*, 1987, **7**, pp. 16–18
16 Oppenheim, A.V., Schafer, R.W.: 'Discrete-time signal processing', (Prentice-Hall, 2009, 3rd edn.)
17 Singer, R.A., Benke, K.W.: 'Real-time tracking filter evaluation and selection for tactical applications', *IEEE Trans. Aerosp. Electron. Syst.*, 1971, **7**, (1), pp. 100–110
18 Maio, A.D., Farina, A., Foglia, G.: 'Target fluctuation models and their application to radar performance prediction', *IEE Proc. Radar Sonar Navig.*, 2004, **151**, (2), pp. 261–269
19 Hao, J., Liu, K., Ren, J., Lu, G., Chen, W., 'IR-UWB radar signal sampling and reconstruction based on step-delay pulses'. Proc. 2011 Int. Conf. on Digital Object Identifier, 2011, pp. 3505–3508
20 Bystrov, A.N.: 'Range finder with stroboscopic signal sampling based on 'Multicore' DSP family', *J. Radio Electron., Gen. Tech. Ser. (Russia)*, 2011, **1**, pp. 107–114